Global asymmetry of fluids and local singularity in the diameter of the coexistence curve

Vitaly B. Rogankov* and Valeriy I. Levchenko
Department of Physics, Odessa State Academy of Refrigeration, 65082 Odessa, Ukraine
(Received 13 June 2012; revised manuscript received 4 April 2013; published 30 May 2013)

By combining a measurable vapor-liquid coexistence curve and the extended van der Waals-type of equation of state (EOS) with the additional temperature-dependent coefficient, the phenomenological model of global fluid asymmetry has been developed separately for both coexisting bulk phases in the entire range of subcritical states. It is shown, in particular, that the adequate description of a liquid branch and its near-critical vicinity in terms of appropriate critical exponents and amplitudes connected by the two-scale-factor universal interrelations can be achieved. The asymmetric influence of heterophase fluctuations on the criticality of gaseous states is demonstrated. It is inherently similar to the well-known Fisher's droplet model, which corresponds to the scaling EOS too. The principle of corresponding *isotherms* has been formulated without any adjustable parameters. An attempt to avoid the use of a locally singular coexistence-curve diameter is proposed in the framework of two alternative models. The accurate vapor-liquid data for two fluid metals, Rb and Cs, as well as two molecular fluids, C_2H_6 and CO_2, are reanalyzed by the above models to confirm the presumed opportunity.

DOI: 10.1103/PhysRevE.87.052141 PACS number(s): 05.70.Jk

I. INTRODUCTION

The terms *global fluid asymmetry* (GFA) and *local singularity* in the coexistence curve (CXC) "diameter" [1] need an explanation if one undertakes the task of converting a cubic (classical) equation of state (EOS) so as to incorporate the near-critical asymptotic behavior [2]. There are two conventional directions of such enlargement which can be conditionally specified as *Ising-model-based* and the *van der Waals (vdW)-fluid-based*. The starting point of the former is the local symmetry of CXC and its fluctuation flattening with the exponent β similar to those observable in the basic lattice-gas model of Ising-like universality. The renormalization group methodology developed mainly by Wilson [3], Fisher [4], and Wegner [5] provides the well-founded theoretical tool for the further extension of scaling concepts in the framework of crossover approach [2].

The alternative way is the vdW-like crossover formalism connected with the names of Fox, Eu, and many others (a brief review of such attempts to incorporate *on an ad hoc basis* the nonanalytic T- and/or ρ-dependent vdW coefficients (a,b) can be found in [2]). The advantages of simplicity and somewhat more realistic values of the critical exponents $\alpha,\beta,\gamma,\delta$ are, however, insufficient to satisfy universality of the known interrelations between the respective critical amplitudes A_0,B_0,C_0,D_0 (see below Table I). One may see that the theoretically based (Ising-like) crossover procedure [2] connects the actual critical point $(P_c,T_c,\rho_c;Z_c=P_c/\rho_c k_B T_c)$ with the fictive mean-field one $(P_c^0,T_c^0,\rho_c^0;Z_c^0=3/8)$, while the vdW-like crossover approach requires further modification to be consistent with the well-established criteria of universality.

The fluctuational-thermodynamic (FT) model [6–8] is an attempt to demonstrate that a third way exists. From the crossover approach one can ask two general questions. Can the original vdW-EOS with two constant coefficients (a,b) provide the realistic information about the actual criticality of real fluids? How can any classical EOS describing exclusively stable one-phase states $(\chi_T>0, C_p>0)$ located outside *its binodal* determine the possible region of anomalous heterophase fluctuations? An affirmative answer, at least to the former question, is achievable by the rejection of a mean-field critical point's concept and by the incorporation of a third constant coefficient c to map the actual values of critical parameters onto the coefficients (a,b,c).

To avoid any ambiguities, the main paths following from the scaling vdW form [6] are represented below, as is the constrained Griffiths' equality (3/2 law) used in FT-EOS [6–8] for the estimate of the remainder (additional to the principal exponent $\beta=1/3$) of the critical FT exponents α,γ,δ from Table I ($\bar{T}=1-T/T_c, \bar{P}=1-P/P_c, \bar{\rho}_i=1-\rho_i/\rho_c$):

$$\text{critical isotherm, } (\bar{T}=0)\ \bar{P}=\pm\left(Z_c^0 A_c^0\right)\ \bar{\rho}^3\Big/\left(1\pm\bar{\rho}/B_0^0\right); \tag{1a}$$

$$\text{critical isobar, } (\bar{P}=0)\ \bar{T}=\mp Z_c^0\bar{\rho}^3\Big/\left(1\mp 2\bar{\rho}/B_0^0\right); \tag{1b}$$

$$\text{critical isochore, } (\bar{\rho}=0)\ \bar{P}=A_c^0\bar{T}; \tag{1c}$$

$$\text{pseudo-CXC, } \bar{\rho}_i=\pm B_0^0\,\bar{T}^{1/2},\ \ \bar{P}=A_c^0\bar{T}; \tag{1d}$$

$$\beta\delta=\beta+\gamma=3/2;\quad \left(B_0^0=2, A_c^0=4,\ Z_c^0=3/8\right). \tag{1e}$$

Despite widespread belief to the contrary, we claim now that both cubic roots of fields $\bar{P},\bar{T}$ in Eqs. (1a) and (1b) play fundamental roles [see Eqs. (29) and (30) below] in the description of actual g branch and l branch, respectively, for realistic CXC. The necessary condition for this aim is the change of any vdW amplitude by its actual counterpart $(B_0,\ A_c,\ Z_c)$, as is demonstrated in Table I. Contrary to the mean-field concept, we consider that Eq. (1d) and its supposed exponent $\beta_0=1/2$ have nothing in common with the realistic (g,l) transition because the equality of chemical i potentials has not been used at its derivation. Thus, the exact exponent $\beta=1/3$ can be defined by Eq. (1b) without any appeal to a Taylor series, at least along the l branch of real fluids.

Obviously, that FT model combines the tasks considered by the theoretically based and phenomenological crossover

*Author to whom all correspondence should be addressed: vrogankov@yandex.ua

TABLE I. Critical exponents and amplitudes accepted by the Ising-like and vdW-like classes of universality for liquidus ($\rho \geqslant \rho_c$) states.

Theory	Exponents	Amplitudes, functions	Interrelations
Scaling [2]	$\alpha = \alpha' = 0.11,\ \rho = \rho_l(T)$	$A_0^+,\ C_v/k_B$	$\frac{\alpha A_0^+ C_0}{B_0^2} = 0.0581$
	$\beta = 0.326$	$B_0,\ \bar{\rho}_l(\bar{T})$	$(\alpha\beta = 0.0359)$
	$\gamma = \gamma' = 1.239$	$C_0^+, \chi_T \rho_l k_B T$	$\frac{C_0^+ D_0}{B_0^{1-\delta}} = 1.57$
	$\delta = 4.8$	$D_0, \bar{P}(\bar{\rho}, T_c)$	$(\beta\delta = 1.565)$
FT model [6–8]	$\alpha' = 1/6, \rho = \rho_l(T)$	$A_0^- = A_c^{2/3}/(3Z_c)$	$\frac{\alpha' A_0^- C_0}{B_0^2} = \alpha'\beta = 1/18$
	$\beta = 1/3$	$B_0 = A_c^{1/3} \approx 1/(2Z_c)$	$A_0^+ \approx B_0/(3Z_c)$
	$\gamma' = 7/6$	$C_0 = Z_c$	$\frac{C_0 D_0}{B_0^{1-\delta}} = \beta\delta' = 3/2$
	$\delta = \delta' = 9/2$	$D_0 = 3/(2Z_c A_c^{7/6})$	

approaches. The former uses the original vdW-EOS to transform it into the scaling EOS by the shift of critical parameters [2],

$$T_c/T_c^0 - 1 = -c_t/8, \quad \rho_c/\rho_c^0 - 1 \approx c_t/54,$$
$$P_c/P_c^0 \approx \left(Z_c/Z_c^0\right)\left(1 - 46c_t/432 - c_t^2/432\right), \qquad (2)$$

where the estimate of the third individual coefficient $c_t(Z_c)$ is based on two phenomenological assumptions. The first one is that far away from T_c the T-dependent CXC diameters of crossover and classical EOSs coincide in the $(T/T_c^0, \rho/\rho_c^0)$ plane (see Fig. 2 in [2]). The second one is that the actual critical point is located below the mean-field critical point but on the same classical vapor-pressure curve $P_\sigma^0(T)$ (see Fig. 3 in [2]). The similar distinctive feature of the FT model is the proven existence of two different reduced slopes: $A_c = (T_c/P_c)(dP_\sigma/dT)_c$ (actual) and $A_c^0 = (T_c/P_c)(dP_\sigma^0/dT)_c = 4$ (classical) *at the same actual value of* Z_c (see Fig. 7 below). It was demonstrated by the FT model that the both slopes generate [6] two alternative sets of critical coefficients:

$$a_c^0 = 3P_c/\rho_c^2; \quad b_c^0 = 1/3\rho_c; \quad c_c^0 = 1 - Z_c/Z_c^0, \qquad (3)$$

$$a_c = P_c(A_c - 1)/\rho_c^2; \quad b_c = (A_c - 2)/[2\rho_c(A_c - 1)];$$
$$c_c = 1 - Z_c A_c^2/[2(A_c - 1)], \qquad (4)$$

related to the *asymmetric behavior* of l and g branches, respectively, *at the same critical point*.

The acceptable correspondence of the phenomenological predictions obtained by the FT model with the well-established results of asymptotic scaling theory [2] in a dense l phase make the further investigation of an asymmetric g phase and of its close one-phase vicinity to be very interesting. The evident indicator of such asymmetry may be the shape of rectilinear CXC diameter and its possible local singularity, which remains a widely debatable problem [9–28]. There are the certain substances in which CXC diameter is strongly curved just to the side of the g phase and, maybe, is singular. This discrepancy with the classical rectilinear shape has been discussed recently by Wang and Anisimov [13] in the framework of complete-scaling methodology developed by Fisher *et al.* [14].

An attempt to avoid the subtle (for real fluids) singularity of diameter with the exponent $(1 - \alpha)$ adopted for the CXC of continuous systems on the base of decorated lattice-gas models has been made in Sec. II. Two phenomenological limiting GFA models are proposed:

(1) regular GFA(r) model with the still rectilinear diameter taking into account the objective experimental errors of CXC data implied especially in the g phase near the critical point;

(2) singular GFA(s) model with the most singular diameter and the admissible divergence of its derivative with the exponent $(-2/3 \approx -2\beta)$.

Both GFA models contain the well-known Guggenheim-Riedel approximation usable in the principle of corresponding *states* [29]. It is applicable to the global description of the entire temperature range for the saturated-liquid density. The alternative examples of a singular diameter (observed in the fluid metals Rb and Cs) as well as of a rectilinear diameter (confirmed experimentally for C_2H_6 and CO_2) have been reanalyzed in Secs. III and IV to compare the GFA models proposed here with the scaling treatment of local singularity in a CXC diameter. It is verified that the account of its rectilinear contribution is the necessary step at the description of global CXC properties, while the singular term with the $(1 - \alpha)$ exponent becomes irrelevant away from the critical point.

It should be stressed that a solution of the crossover problem proposed by the FT model,

$$\frac{T_c}{T_c^0} = \frac{27A_c^2(A_c - 2)}{32(A_c - 1)^3}, \quad \frac{\rho_c}{\rho_c^0} = \frac{3(A_c - 2)}{2(A_c - 1)},$$
$$\frac{P_c}{P_c^0} = \frac{27(A_c - 2)^2}{4(A_c - 1)^3}, \quad \frac{Z_c}{Z_c^0} = \frac{16(A_c - 1)}{3A_c^2}, \qquad (5)$$

looks similar to that expressed by Eq. (2), only formally. The fictive mean-field stable critical point considered in [2] at (Z_c^0, A_c^0) is absent. The classical denotations of critical parameters in Eq. (5) are related to the predicted *unstable critical point* of the FT model. The respective nonclassical pseudospinodal starts at the actual critical point and goes up to this point in the (P,T) plane. It is completely located at the gaslike ($\rho \leqslant \rho_c$) densities (Sec. V) of a supercritical region ($T \geqslant T_c$).

II. TWO TRENDS OF (*g*,*l*) ASYMMETRY IN THE RECTILINEAR CXC DIAMETER

The empirical law of rectilinear diameter formulated long ago by Cailletet and Matthias [1] for two branches, $\rho_g(\bar{T})$ and

$\rho_l(\bar{T})$, of CXC, where $\bar{T} = 1 - T/T_c$,

$$\rho_d^* \equiv (\rho_g + \rho_l)/2\rho_c = 1 + D_1\bar{T}, \tag{6}$$

is at variance with the perfect asymptotic symmetry of the lattice gas [2]:

$$\bar{\rho}_i \equiv \rho_i/\rho_c - 1 = \pm B_0\bar{T}^{\beta}, \tag{7a}$$

$$\rho_d^* = 1, \tag{7b}$$

where $i = l$ or g, respectively, for the *homophase order parameters* $\bar{\rho}_i$. The equality for the *heterophase order parameter* $\Delta\bar{\rho}$ which coincides with that for its homophase counterpart $\bar{\rho}_l$ in orthobaric liquid from Eq. (7a) describes an asymptotic symmetry:

$$\Delta\bar{\rho} \equiv (\rho_l - \rho_g)/2\rho_c = B_0\bar{T}^{\beta} + \cdots. \tag{8}$$

The additional important equality for the above difference of CXC densities $\Delta\bar{\rho}$ has to be fulfilled to achieve the consistency with the thermodynamic Clapeyron's equation. It is expressed here in terms of the reduced slope taken along a measurable vapor-pressure curve, $A_\sigma = (T/P_\sigma)(dP_\sigma/dT)$, and the compressibility factor, $Z_l = P_\sigma/(\rho_l k_B T)$, of orthobaric liquid,

$$\Delta\bar{\rho} = \frac{(s_g - s_l)\rho_g}{2k_B A_\sigma Z_l \rho_c}, \tag{9}$$

where s_i is the orthobaric specific entropy determined per particle (per mole, per unit of mass). At the actual critical point (P_c, ρ_c, T_c) of a fluid one obtains the only asymptotic trend [6–8],

$$\Delta\bar{\rho} = \Delta\bar{s}/(A_c Z_c)_{\Delta\bar{\rho},\Delta\bar{s}\to 0}, \tag{10}$$

where the appropriate definition of the *heterophase disorder parameter* has been introduced:

$$x \equiv \Delta\bar{s} = (s_g - s_l)/2k_B. \tag{11}$$

This quantity must have the same type of asymptotic behavior as the heterophase order parameter $\Delta\bar{\rho}$ from Eq. (8) if the scaling assumptions are consistent and adequate in the $(\bar{T},\bar{\rho})$ plane.

The spectacular nonanalyticity and asymptotic symmetry (but found [6–8] in the $(x,\bar{\rho})$ plane at $x \leqslant 0.5$) for the real fluids (Ar, C_2H_4, CO_2, H_2O) as well as for the original vdW-EOS is shown in Fig. 1. The coefficient from Eq. (10) for this model of a fluid is $1/(A_c^0 Z_c^0) = 2/3$, while the respective disorder parameter becomes classical, $x^0 \equiv \Delta\bar{s}^0$. Nevertheless, the vdW model demonstrates the nearly perfect CXC symmetry with zero slope of "diameter" if the $\Delta\bar{s}$ quantity is used instead of variable $\bar{T}$. The asymptotic non-mean-field behavior of both global CXC branches implied by the common *curvilinear* (with an inflection point at $x \approx 2$) *but regular diameter*: $[\rho_d^*(x)]_{x\to 0} \to 1$, $[d\rho_d^*/dx]_{x\to 0} \to 0$ *becomes an explainable result*. The observation of its S shape in a combination with the obvious nonanalyticity of both (intercrossing) CXC branches following from Fig. 1 gives a possibility to formulate here the *hypothesis about the existence of a wide vdW-like class of GFA including the critical universality for real fluids*. For confirmation (or rejection) of it one should not distort the original vdW EOS by the mean-field analytic interpretation as well as apply the Wegner's nonanalytic expansion.

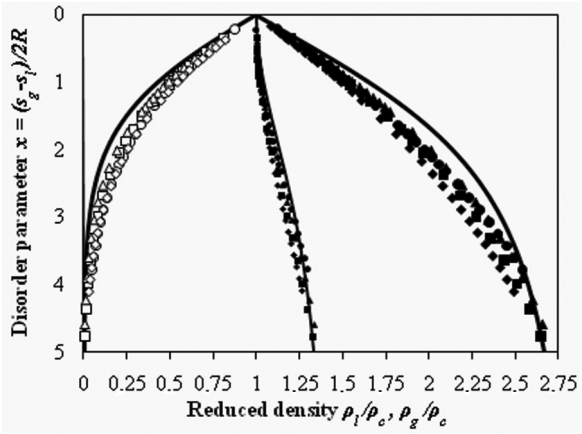

FIG. 1. vdW-like universality and the GFA of real substances. Comparison of the reduced CXC-densities $\rho_{l,g}/\rho_c$ for real substances: Ar (triangles), C_2H_4 (squares), CO_2 (diamonds), H_2O (circles) with the vdW-Maxwell-Gibbs model's predictions (solid line) based on the disorder parameter x [6]. The characteristic S-shape of CXC diameter $(\rho_l + \rho_g)/2\rho_c$ and its regular (tangential to the critical isochore ρ_c) local near-critical behavior become evident at the replacement of temperature $\bar{T} = 1 - T/T_c$ by the heterophase disorder parameter x.

The most striking feature of the above hypothesis illuminated by the FT model and by the respective FT-EOS is the consistency of the most accurate experimental CXC data $[\rho_g(T),\ \rho_l(T),\ P_\sigma(T)]$ for a variety of real fluids, simultaneously, with two different ratios of nonclassical, $x(T)/A_\sigma(T)$, and classical, $x^0(T)/A_\sigma^0(T)$, parameters in the framework of Clapeyron's Eq. (9). The existence of two different functionals [6–8] $P_\sigma[\rho_g(T)]$ and $P_\sigma^0[\rho_g(T)/\rho_l(T)]$ for any CXC was proven. Its asymptotic form expressed by Eq. (10) demonstrates two alternative near-critical trends either in the disorder parameter $\Delta\bar{s}$ or in the reduced slope A_σ.

The combination based on the known Guggenheim-Riedel approximation [29],

$$\bar{\rho}_i = \pm B_0\bar{T}^{1/3} + D_1\bar{T}, \tag{12}$$

is often usable for the global description of CXC with the restriction $B_0 = A_c^{1/3}$. One of the goals below is to demonstrate the shortcomings of the conventional local approach at the global representation of measurable CXC data. The known problem is that both contributions of the singular and regular ρ_d^* behavior cannot be unambiguously separated and must have opposite signs. An attempt to avoid the use of the $(1-\alpha)$ term has been performed below for the vdW-like systems.

The most detailed study of local ρ_d^* singularity was performed by Wang and Anisimov [13] in the framework of the Fisher's complete scaling [14]. One may note an appearance of the additional singular terms in a combination with the same Eq. (8):

$$\rho_d^* = 1 + D_0\bar{T}^{1-\alpha} + D_1\bar{T} + D_2\bar{T}^{2\beta}, \tag{13}$$

$$\bar{\rho}_i = \pm B_0\bar{T}^{\beta} + D_0\bar{T}^{1-\alpha} + D_1\bar{T} + D_2\bar{T}^{2\beta}. \tag{14}$$

Let us remember that the concept of local ρ_d^* singularity divides, as a matter of fact, the Ising-like systems into the certain subclasses of universality with the *observable* curvilinear or rectilinear variants of local ρ_d^* behavior. Wang

and Anisimov [13] proposed the smart explanation of a system-dependent distinction by the possible compensation of nonanalytic contributions in Eqs. (13) and (14) when the description by Eqs. (6), (8), and (12) becomes adequate. In such a case, the signs of D_1, D_2 are mainly positive while the sign of D_0 is negative, the opposite of the suppositions of authors [9,23], for example. The very small size of the D_2 amplitude estimated by Hensel and co-workers [9] for liquid metals in the much wider range of temperature $10^{-3} < \bar{T} < 10^{-1}$ needs also an explanation.

The FT model was described in full detail [6–8,15,16], so we only include here its reduced predictive form obtained by the elimination of dimensional FT coefficients:

$$\pi[\varphi(T)] = \frac{\varphi\{A[1 + C(1-\varphi)] - B[1 + C(1-\varphi^2)]\}}{A - B\varphi}, \tag{15}$$

where all T-dependent parameters and the universal coefficients are well-defined in both of the coexisting phases by the input CXC data. So the reduced pressure is $\pi = P(T)/P_\sigma(T) \leqslant 1$ at any chosen temperature in a one-phase subcritical gas where the reduced density, $\varphi = \rho(T)/\rho_l(T)$, must be less ($\varphi \leqslant \varphi_\sigma$) than its CXC value, $\varphi_\sigma = \rho_g(T)/\rho_l(T)$. The reduced parameters in a one-phase liquid are, respectively, $\pi = P(T)/P^0_\sigma(T) \geqslant 1$ and $\varphi \geqslant 1$. The universal coefficients are positive:

$$A(T) = \varphi_\sigma(1 + \varphi_\sigma)(A_\sigma - 1) > 0, \tag{16}$$

$$B(T) = \varphi_\sigma(A_\sigma - 2) > 0, \tag{17}$$

$$C(T) = (A_\sigma - 1)/\varphi_\sigma > 0. \tag{18}$$

Any adjustable coefficients are absent because the classical (but non-mean-field) bubble-point curve P^0_σ and its reduced slope A^0_σ from Eqs. (16)–(18) are also exactly determined [15,16] by the FT-converting of input CXC data.

The distinction of reduced FT-EOS (15)–(18) from the conventional variants of corresponding *states* principle [29] is evident. The reduced parameters π, φ are determined here by the *entire CXC* instead of a *single critical point* usable for this aim in the standard methodology. One may consider such a functional of the reduced density $\pi[\varphi(T)]$ (15) depending on the subcritical temperature as the corresponding *isotherms* principle. The impressive GFA of Eqs. (15)–(18) is related to the difference between the supposed classical bubble-point curve $P^0_\sigma(T)$ in l phase and the measurable (input) dew-point curve $P_\sigma(T)$ in g phase.

The dimensional form of FT-EOS [15,16] can be used to estimate the global difference between the nonclassical and classical trends in the CXC diameter:

$$\frac{d\rho_d}{dT} = -\frac{1}{2b^2}\frac{db}{dT} - \frac{A_\sigma}{2bT(A_\sigma - 1)} + \frac{1}{2b(A_\sigma - 1)^2}\frac{T}{P_\sigma}\frac{d^2P_\sigma}{dT^2}. \tag{19}$$

Both are determined by the existence of two alternative pairs of coefficients, (b, A_σ) and (b^0, A^0_σ), respectively, *for the same input CXC data*. From a physical viewpoint, such opportunity is explainable by the significant distinction (asymmetry) in the molecular behavior and structure of coexisting g and l phases. This difference is expressed here by the effective T-dependent sets of coefficients: $(a,\ b,\ c,\ A_\sigma)$ and $(a^0, b^0, c^0, A^0_\sigma)$. The high predictive ability of Eqs. (15)–(18) in one-phase regions has been confirmed earlier for the wide class of different subcritical fluids (Ar, N_2, CO_2, NH_3, H_2O, ..., hydrocarbons, CH_4, C_2H_2, C_2H_4, C_2H_6, ..., alcohols, CH_3OH, C_2H_5OH, ..., ionic liquids, liquid metals, Rb, Cs, ..., etc.). The stable and metastable properties of gas were predicted by the nonclassical set of FT-EOS coefficients while those for liquid were predicted by the classical set. Interesting consequences of global asymmetry [8,15,16] are observable in the vicinity of critical point where distinctions in the coexisting phases must disappear in accordance with its classical description.

The necessary ingredients of both proposed phenomenological GFA models are

(1) the contribution of rectilinear diameter;

(2) the elimination of its asymptotic singularity with the $(1 - \alpha)$ exponent.

We consider that the presence of the latter can be rigorously confirmed only for the determinate models discussed earlier while, within the experimental CXC uncertainties, it is simply the plausible supposition. The objective difference in the accuracy at the measurements [10] of orthobaric densities $\rho_g(T)$ and $\rho_l(T)$ must be taken into account in the estimates of asymptotic ρ^*_d singularity.

To compose the first phenomenological (regular) GFA(r) model we propose to use Eqs. (6), (8), and (12) as its consistent determinate background. It is convenient to fix below the amplitude B_0 the Riedel condition, $B_0 = A_c^{1/3}$, and *to adjust*, then, the consistent value D_1. The following requirement seems natural if one takes into account the good correspondence of the Guggenheim-Riedel Eq. (12) with a positive sign in front of B_0 to the experimental $\rho_l(T)$ data for any substances. We propose the choice of D_1 based on the conjecture that the systematic (experimental) deviations of densities, $\delta_l = |\rho_l/\rho_l^{\exp} - 1| < \delta_g = |\rho_g/\rho_g^{\exp} - 1|$, must be, respectively, positive in l phase and negative in g phase at any subcritical temperatures. This choice is mainly an attempt to take into account the unavoidable phenomenon of precondensation which increases the measured value of $\rho_g^{\exp}(T)$ [10], especially at the near-critical temperatures. The crucial step to formulate the regular GFA(r) model is the adjustment of two dimensionless parameters of *shift*, $\varepsilon = \delta_l$, and *asymmetry*, $k = \delta_g/\delta_l$, for the reasonable representation of experimental CXC data:

$$\bar{\rho}_l = B_0\bar{T}^{1/3} + D_1\bar{T} - \varepsilon\rho_l^{\exp}\big/\rho_c, \tag{20}$$

$$\bar{\rho}_g = -B_0\bar{T}^{1/3} + D_1\bar{T} + k\varepsilon\rho_g^{\exp}\big/\rho_c, \tag{21}$$

$$\rho^*_d = 1 + D_1\bar{T} + \varepsilon\big(k\rho_g^{\exp} - \rho_l^{\exp}\big)\big/2\rho_c, \tag{22}$$

$$\Delta\bar{\rho} = B_o\bar{T}^{1/3} - \varepsilon\big(k\rho_g^{\exp} + \rho_l^{\exp}\big)\big/2\rho_c. \tag{23}$$

The assumptive inconsistency between the left and right sides at the critical point itself $\bar{T} = 0$ imitates here the existence of actual uncertainty $\delta_c = \rho_c/\rho_c^{\exp} - 1$ at the determination of the ρ_c value by the rule of rectilinear diameter [13]. One has to ignore this realistic uncertainty only in the asymptotic range $\bar{T} \leqslant 10^{-3}$ by the assumption $\varepsilon = k = 0$ in Eqs. (20)–(23) (Sec. IV).

The second phenomenological (singular) GFA(s) model has the same determinate background formed by Eqs. (6), (8), (12)

exclusively if the special conditions of symmetry, $D_1^l = D_1^g = D_1$ and $B_0 = 2D_1$, for amplitudes are fulfilled in the following system of equalities:

$$\bar{\rho}_l = D_1^l(\bar{T} + 2\bar{T}^{1/3}), \tag{24}$$

$$\bar{\rho}_g = D_1^g(\bar{T} - 2\bar{T}^{1/3}), \tag{25}$$

$$\rho_d^* = 1 + \left(D_1^l + D_1^g\right)\bar{T}/2 + \left(D_1^l - D_1^g\right)\bar{T}^{1/3}, \tag{26}$$

$$\Delta\bar{\rho} = \left(D_1^l - D_1^g\right)\bar{T}/2 + \left(D_1^l + D_1^g\right)\bar{T}^{1/3}. \tag{27}$$

These conditions can be approximately satisfied for the substances with the actual rectilinear diameter such as CO_2 or C_2H_6 (Sec. IV). The noticeable difference of GFA(s) model even from the concept of local ρ_d^* singularity in the complete scaling described by Eqs. (8), (13), and (14) is quite essential. Indeed, the derivative $d\rho_d^*/d\bar{T}$ from Eq. (26) has the much stronger (limiting) divergence than that following from Eq. (13). Such singularity may be masked in the substances with the rectilinear diameter, where $D_1^l \approx D_1^g$ and becomes crucial if D_1^l is larger than D_1^g.

III. UNIVERSALITY OF COEXISTENCE CURVE IN FLUID METALS

Once the CXC data $[P_\sigma(T), \rho_g(T), \rho_l(T)]$ are measured one may investigate to what extent the shape of the T dependencies (1) matches the expected asymptotic near-critical behavior and (2) is the thermodynamically consistent. Unfortunately, the widespread approach is the study of first problem mainly in the (T,ρ) plane while the second one remains "shadowed." The presumed difference between the criticality of molecular and ionic fluids [18,19] requires for its confirmation just the consideration of both problems. However, the respective vapor-pressure data $P_\sigma(T)$ in the near-critical region are rather scarce. The situation with respect to a possible transformation of the critical exponents into the so-called "near-mean-field" ones for ionic fluids remains inconclusive.

In this context, an application of GFA models can provide the additional arguments *pro et contra* of the above distinction in the criticality of molecular and ionic fluids. One may note that the impressive curvature of the CXC diameter found in Rb and Cs [9] has been observed [13] also experimentally in such molecular fluids as SF_6 [20] and $C_2F_3Cl_3$ [21]. At the same time, the other authors [22] have considered the respective scaling treatment of measured near-critical CXC data for SF_6 in [20] as debatable. We do not also dwell any further on the issue of analytic criticality supposed [29] in the fluid metals. There are two reasons for such caution:

(1) authors [9] claimed the usage of $P_\sigma(T)$ data for Rb and Cs but neither reported these values nor represented the orthobaric densities ρ_g, ρ_l *at the equal temperatures*;

(2) we consider the nonanalytic exponent, $\beta = 1/3$, in Eq. (12) determined for *both CXC branches far away from the critical point as the fundamental universal parameter of any vdW-like fluids including ones with the relatively long-range interactions*.

Hence, it is impossible to use directly the FT model's treatment for a fluid metal. It needs the input $P_\sigma(T)$ data too. Another consequence is that the alternative mean-field's variant of CXC description with the exponent $\beta_0 = 1/2$ supposed for all alkali fluid metals in the framework of thermodynamic similarity [29] is omitted in the present work (see also our earlier work [24] on the problem of Rb and Cs) as highly modelistic. The aim below is to demonstrate the crucial role of rectilinear ρ_d^* diameter even in such fluids with a striking CXC asymmetry as fluid metals.

There were many interesting attempts [2,13,17–19, 22,25–28] to connect the system-dependent amplitudes (B_0, D_0, D_1, D_2) with the different characteristics of molecular structure, polarizability, electric conductivity, fictitious diameter, and the well depth of effective interactions. The use of measurable critical quantities (A_c, Z_c) and other parameters of thermodynamic similarity such as the Pitzer's acentric factor [28] *based on the vapor-pressure* $P_\sigma(T)$ *data* is the appropriate "bridge" in the search for this connection. It is also desirable to search for the above correlations within the common universality classes similar to Ising-like or vdW-like ones summarized in Table I.

Thus, the correlation of two asymptotic amplitudes, $B_0 = A_c^{1/3}$, adopted in the concept of both GFA models has to be conjugated with the universal set of exponents ($\alpha = 1/6$, $\beta = 1/3$, $\gamma = 7/6$, $\delta = 9/2$), which are close to the best scaling estimates [2,13] ($\alpha = 0.11$, $\beta = 0.326$, $\gamma = 1.239$, $\delta = 4.8$) accepted for Ising-like systems. Then one may consider the amplitude D_2 (its role is discussed in detail by authors [13] for molecular substances) as well as the amplitude D_1 from the remaining ones (D_0, D_1) (taking into account the possible correlation $D_1 = B_0 - 1$ in Eq. (12) [29]) as adjustable parameters. Since these amplitudes (D_0, D_1) in Eqs. (13) and (14) are strongly correlated [13] and, additionally, may have the different signs, it seems preferable, first of all, to choose the positive amplitude D_1 of a linear ρ_d^* contribution. The results for Cs are represented in Table II and shown in Fig. 2 to demonstrate the GFA(r) methodology in a step-by-step manner. Its main advantage is the simplicity and the applicability to the entire range of subcritical temperatures. Its constraint is an *a priori* supposed uncertainty at the determination of actual critical density ρ_c as it is shown in Fig. 6 for ethane. The trial and error method used below contains the following steps.

Hensel and co-workers [9] have fitted on exclusively the nonanalytic amplitudes B_0, D_0 (Table II) by the scaling approximation but have not reported just the contribution D_1 of rectilinear diameter. Besides, the so-called "confluent singularity" [2] with the exponent $(1 - \alpha + \Delta)$ was supposed. Our attempt to use the above-mentioned approximation $D_1 = B_0 - 1$ [29] far enough from the critical point (without the confluent contribution) was unsuccessful. Then we have fixed the amplitude $B_0 = 2.25$ [9] and omitted the singular contribution with the exponent $(1 - \alpha)$ to study the applicability of original approximation [29] developed by Guggenheim and Riedel for l branch:

$$\bar{\rho}_l = 0{,}85\bar{T} + (0{,}53 + 0{,}2A_c)\,\bar{T}^{1/3}, \tag{28}$$

where $A_c = B_0^3 = 11{,}39$. One may note that the interpretation of Eq. (28) in terms of Eq. (24) [GFA(s) model] at the assumption $D_1^l = 0.85$ gives the significantly different estimates, $A_c = 5.85$ (close to the argon's one) and

TABLE II. Critical parameters, exponents, and CXC amplitudes used by Hensel and co-workers [9] to fit the experimental data for Cs and Rb in comparison with the reanalyzed description based on the GFA models (see Figs. 2–5).

Cesium [9]	$T_c = 1924$ K; $P_c = 9.25$ MPa; $\rho_c = 0.379$ g/cm^3; $Z_c = 0.2028$
CXC-fit [9]	$B_o = 2.25$; $D_o = 2.1$; $\alpha = 0.13$; $\beta = 0.355$
GFA(r)	$B_o = 2.25$; $D_1 = 2.6$; $\varepsilon = 0.01$; $k = 7$; $A_c = 11.39$
GFA(s) [24]	$B_o = 2.167$; $D_1 = 1.0835$; $D_1{}^l = 1.205$; $D_1{}^g = 0.962$
FT(T_c)	$a_c{}^o = 3412.6$ J dm^3/mol^2; $b_c{}^o = 0.1169$ dm^3/mol; $1 - c_c{}^o = 0.54075$
Rubidium [9]	$T_c = 2017$ K; $P_c = 12.45$ MPa; $\rho_c = 0.292$ g/cm^3; $Z_c = 0.2173$
CXC fit [9]	$B_o = 2.45$; $D_o = 2.3$; $\alpha = 0.14$; $\beta = 0.360$
GFA(s) [24]	$B_o = 2.242$; $D_1 = 1.121$; $D_1{}^l = 1.316$; $D_1{}^g = 0.926$
FT(T_c)	$a_c{}^o = 3200$ J dm^3/mol^2; $b_c{}^o = 0.097\,57$ dm^3/mol; $1 - c_c{}^o = 0.57947$

$B_0 = A_c^{1/3} = 1.802$, when the correlation [29], $D_1 = B_0 - 1$, is approximately fulfilled. However, Eq. (28) itself and its symmetric counterparts [Eqs. (24)–(27)] obtained from the GFA(s) model at the condition $D_1^l = D_1^g = D_1 = 0.85$ do not provide the satisfactory description of CXC data [9] for Cs.

The described unpromising results forced us, first, to use the correlation (12) with the same fixed $B_0 = 2.25$ value from [9] but with the free amplitude parameter D_1 of rectilinear contribution as the background for the GFA(r) model. The chosen value $D_1 = 2.6$ (Table II) guarantees just the necessary shape of an outer curve shown in Fig. 2 by the dotted line. It is obvious that the standard correlation [29], $D_1 = B_0 - 1$, fails now completely for the highly asymmetric shape of CXC.

At the same time the parameters of shift assumed here, $\varepsilon = 0{,}01$, and asymmetry, $k = 7$ (Table II) provide excellent representation of both (g,l) branches and the ρ_d^* diameter (Fig. 2) up to the immediate neighborhood of the critical point by the GFA(r) Eqs. (20)–(23).The ε parameter was chosen as the maximum relative error at the measurements of orthobaric densities reported by authors [9]. The comparatively large k parameter reflects, presumably, the great volume change observable in any ionic fluids. Let us recall, once more, that the incorporation of these adjustable parameters on the right-hand sides (rhs) of Eqs. (20)–(23) must imitate an *unmeasurable but realistic* redistribution of orthobaric masses between the above volumes implied by the phenomenon of pre-condensation.

The essential feature of both GFA models is an absence of the singular $1 - \alpha$ term and the presence of linear term in the CXC diameter. From our viewpoint, the similarity of chosen values for the main subcritical amplitude B_0 (2.25 and 2.167 for Cs in Table II; see also Fig. 3) confirms the physical adequacy of both GFA models. The sharp discrepancy between the respective D_1 amplitudes (2.6 and 1.0835 for Cs in Table II) gives a possibility to represent the observable global asymmetry for any substance, including the fluid metals in term either (ε,k) parameters or (D_1^l, D_1^g) amplitudes. In this rather principled meaning, the vdW-like universality is wider than the Ising-like universality in which a "near-mean-field" concept of criticality is often necessary for the liquid metals [29].

The predicted GFA(r)-model values are not represented in Table II for Rb because the fitted amplitude $B_0 = 2.45$ [9] ($A_c = B_0^3 = 14.71$) seems strongly overestimated. To obtain

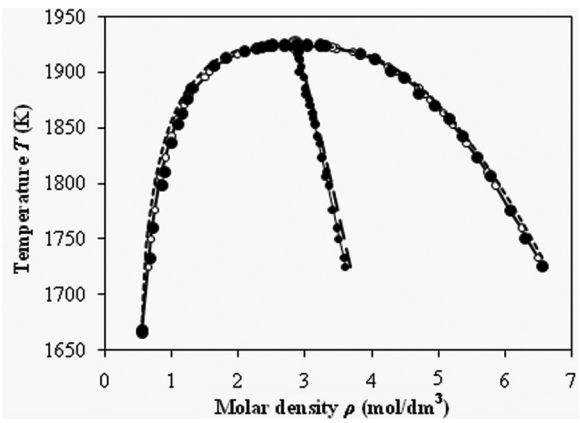

FIG. 2. Reanalyzed by the GFA(r) model (Table II) CXC data for Cs [9] with the omission of nonanalytic $(1 - \alpha)$ contribution usable at the scaling treatment of the near-critical experiment; large black circles, experimental points [9]; small white circles, quasiexperimental points predicted at the same subcritical temperatures by Eqs. (20) and (21); small black circles, ρ_d^* diameter's points predicted as a half sum of the actual [9] and quasiexperimental (present work) points; the dotted line represents the preliminary fit by Eq. (12) (see text); the dashed line is the extrapolated singular ρ_d^* diameter [9], which is shown for comparison with the GFA(r) model's results.

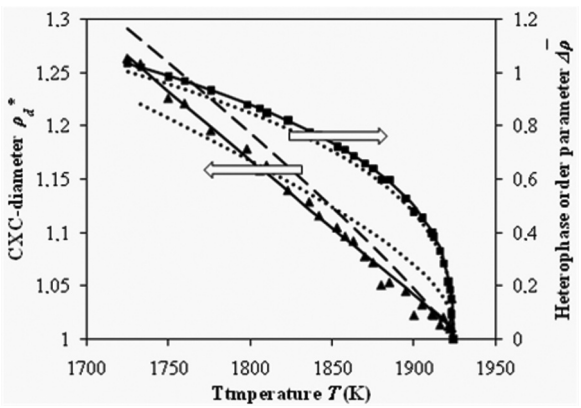

FIG. 3. Comparison (left scale) of the extrapolated (presumably, with the existence of a Wegner-type correction) CXC diameter for Cs [9] (dashed line), with its GFA(r) variant (solid line) and the GFA(s) variant (dotted line); symbols are the quasiexperimental points (triangles) determined as a half sum for the actual measured ρ_i values ($i = l$ or g) [9] and the GFA(r) values predicted for the opposite side of CXC at the same temperature. Comparison of the respective heterophase order parameters (right scale); the quasiexperimental points are shown here by the squares.

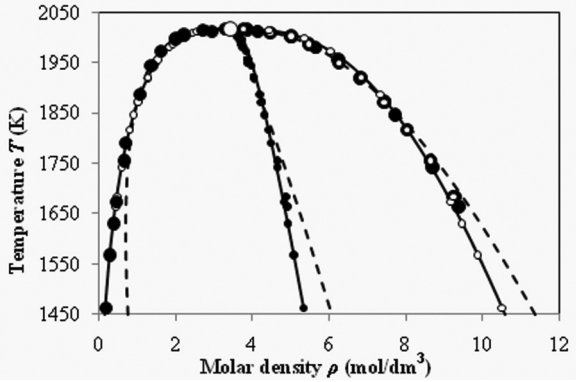

FIG. 4. Reanalysis by the GFA(s) model (Table II) CXC data for Rb [9] with the omission of the nonanalytic $(1-\alpha)$ contribution usable at the scaling treatment of near-critical experiment. Symbols and lines are the same as those shown in Fig. 2.

the more realistic estimate of critical slope A_c (the Riedel factor of thermodynamic similarity) we have used the GFA(s) model as is shown in Fig. 4 and represented in Table II. Its preferableness far away from the critical point at $\bar{T} \geqslant 5 \times 10^{-2}$ is obvious while the extrapolated singular behavior of ρ_g branch [9] at $B_0 = 2.45$; $\beta = 0.360$ looks here anomalous. Taking into account the thermodynamic similarity of Rb and Cs as well as the closeness of critical GFA(s) amplitudes following from Table II one may consider the respective near-critical values of density $\rho_g(T)$ to be reliable in spite of the some systematic deviations from experimental data [9].

The hypothesis of vdW-like universality and the phenomenological GFA models provide the unique possibility to test the consistency of any experimental CXC data by the reconstruction [15,16] of a dew point's functional $P_\sigma[\rho_g(T)]$ (see Fig. 5) *calculated at the actual critical temperature* T_c

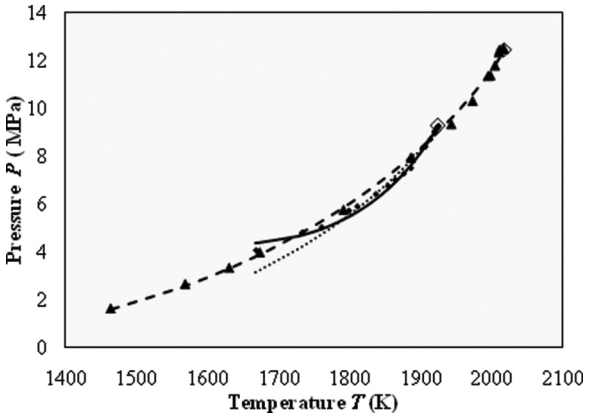

FIG. 5. Vapor-pressure curves (dew point's functionals of the orthobaric vapor densities $P_\sigma[\rho_g(T)]$) predicted (see text) for Cs by the GFA(r) model (solid line) and by the GFA(s) model (dotted line), as well as for Rb by the GFA(s) model (dashed line). The quasiexperimental $P_\sigma[\rho_g(T)]$ points shown by symbols (small diamonds for Cs and large triangles for Rb) are calculated by the same Eqs. (2) and (29) on the basis of the orthobaric vapor densities measured by Hensel *et al.* [9]. The respective critical points are shown by the open symbols.

with the classical FT coefficients from Eq. (3):

$$P_\sigma[\rho_g(T)] = \frac{\rho_g R T_c \left(1 - c_c^0\right)}{1 - b_c^0 \rho_g} - a_c^0 \rho_g^2. \tag{29}$$

This result demonstrates explicitly the special role of a classical critical isotherm as the envelope in the (P,ρ) plane of the whole family of subcritical isotherms starting in the one-phase classical liquid. Hence, in such context the conventional concept of unified EOS fails because one cannot apply to such a family the standard Maxwell's rule and to determine, simultaneously, the total set of binodal CXC data $[P_\sigma(T)$, $\rho_g(T)$, $\rho_l(T)]$. Only the location of the critical point and one of the T dependences $[\rho_g(T)$ or $P_\sigma(T)]$ has to be known to reconstruct the second one by Eq. (29).

The dew point's trend has the bubble point's trend counterpart [15,16] generated by the nonclassical T-dependent FT-EOS coefficients taken along the *nonclassical critical isobar*:

$$P_c = \frac{\rho_l R T (1 - c)}{1 - b\rho_l} - a\rho_l^2. \tag{30}$$

It is presumably the *envelope in the* (T,ρ) *plane of the whole family of subcritical isobars starting in the one-phase nonclassical gas*. One must know [30] the above total set of CXC data to test this correlation. The striking GFA manifestation, as well as the principal distinction between the critical isotherm and the critical isobar, become obvious in the framework of the FT model. Let us remember that both critical paths above are considered as *strong* ones in the conventional terminology of criticality proposed by Griffiths and Wheeler. On the other hand, the FT model predicts the existence of *two* special *weak* directions of $P_\sigma(T)$ and $P_\sigma^0(T)$ curves (see below, Fig. 7) while this terminology postulates the only $P_\sigma(T)$ direction that is singled out at $T \leqslant T_c$ and $T > T_c$.

It is seen from Fig. 5 that the quasiexperimental vapor pressures (shown by symbols) calculated by Eq. (29) for Rb and Cs are located relatively close to ones shown by the smooth curves and based on the $\rho_g(T)$ values predicted by the GFA models. One may notice the significantly less curvature of both $P_\sigma(T)$ functions predicted by the GFA(s) model in comparison with that for Cs based on the GFA(r) predictions. Just the latter model will be used for the well-studied substances CO_2 and C_2H_6 in Sec. IV. At the same time, the GFA(s) model provides the reliable prediction of quasiexperimental pressures for Rb at lower temperatures, $T \leqslant 1800$ K. We consider that the experimental $\rho_g(T)$ points [9] for Rb in this range need the correction at which the GFA(r) model should become applicable to the entire temperature range $1450 \leqslant T \leqslant T_c$. In any case, the adequate description of the experimental $\rho_g(T)$ data by the GFA model is a guarantee of a reliable prediction of the $P_\sigma[\rho_g(T)]$ data by the FT model's Eq. (29). The verification of Eq. (30) is the complicated task for Rb and Cs since the set of CXC data reported by Hensel and co-workers [9] is not complete.

IV. THERMODYNAMIC CONSISTENCY OF ORTHOBARIC DENSITIES WITH THE VAPOR PRESSURE FOR ETHANE AND CARBON DIOXIDE

The study of C_2H_6 performed long ago [10] and the similar, even earlier, study of CO_2 [31] remain until now the standard of careful experimental investigation in the region of (v,l) transition including the near-critical vicinity. The high quality of simultaneous measurements of densities $[\rho_g(T),\rho_l(T)]$ and pressure $P_\sigma(T)$ provides the reliable basis to test below the predictive efficiency of the FT model. It was used in Sec. III for Rb and Cs at the reconstruction of the vapor-pressure curves. Another aim is here to estimate the artificial consequences originated by the several widespread methodologies of CXC fit used, in particular, by the authors of Refs. [10,31].

The noticeable one is the inconsistent combination of the rectilinear-diameter rule (6) and the heterophase order parameter (8) with the (ill-founded in the critical region) extrapolated low-temperature Clapeyron-Clausius equation,

$$\lg P_\sigma = -875.186/T + 4.73909, \tag{31}$$

chosen for CO_2 by Michels and coauthors [31]. As a result, the formal possibility to fit reasonably (see the respective column in Table IV) on the measured vapor pressure by Eq. (31) in the limited range of temperature considered in [31] may give the serious discrepancies in the value of the Riedel factor A_c. In particular, its approximate estimate by two calculated pressures (critical and the closest to it) provides the unrealistic value $A_c = 18.1$, while the experimental slope [31] for the same temperatures (304.19 K and 304.1 K) is $A_c = 8.196$. Since the halves of orthobaric sum ρ_d^* and difference $\Delta\bar{\rho}$ may be transformed into the empirical variant (12) for the homophase order parameters $\bar{\rho}_i$ one can apply the same amplitudes B_0, D_1 from Table III to the description of both CXC branches, separately. However, even the more realistic critical slope, $A_c = B_0^3 \approx 7.55$, in the accepted combination with the other empirical slope, $D_1 = B_0 - 1 \approx 0.9618$, do not provide, in this case, the reasonable accuracy of description. The direct application of amplitudes taken from [31] gives the large systematic deviations (Table IV) at the description of orthobaric densities for CO_2.

To improve the situation we have developed the purely predictive variant of GFA(r) model based on the only input parameter $A_c = 7.044$ taken from the very accurate CXC data [32] and verified [6] in the framework of the FT model. The relevant amplitudes and GFA(r) parameters are represented in Table III. We have used the values of densities $\bar{\rho}_i$ previously predicted by Eq. (12) instead of the unsmoothed experimental values $\bar{\rho}_i^{\exp}$ [31] in Eqs. (20)–(23). However, the measured CXC data were also utilized to predict the vapor pressure $P_\sigma(T)$ by Eq. (29). In spite of the small systematic deviations from the experimental data [31], the FT methodology of the $P_\sigma[\rho_g(T)]$ functional provides the excellent level of predictive ability. The main condition for such a promising result is the reliable description of the input $\rho_g(T)$ data. The GFA(r) model corresponds (Table IV) to this requirement, contrary to the original CXC fit [31].

Sengers and co-workers [33] used the same experimental basis [31] at the development of crossover model from *singular critical* to *regular classical* behavior of CO_2 fluid in the relatively narrow ranges of temperature ($298\ \mathrm{K} \leqslant T \leqslant T_c$) and density ($5.57\ \mathrm{mol/dm^3} \leqslant \rho \leqslant 13.64\ \mathrm{mol/dm^3}$). It should be noted that both *unified* nonanalytic and analytic types of EOS (such as those developed for C_2H_6, respectively, in [23] and [34]) do not provide the agreement with the accurate volumetric measurements of liquid [10] at the near-critical (or lower) temperatures and at the higher densities [23]. In contrast, the classical FT model gives the *reliable prediction of liquids up to the critical temperature and at the highest experimental densities*.

In the frameworks of GFA models both (nonanalytic and regular) contributions in Eq. (12) are essential everywhere along the entire CXC. It follows from Table IV that the GFA(r) description should be replaced by the asymptotic (at $\varepsilon = k = 0$) singular Eq. (12) for CO_2 only in the immediate vicinity ($303\ \mathrm{K} \leqslant T \leqslant 304.19\ \mathrm{K}$) of T_c. In the much wider range of temperatures the thermodynamically consistent predictions by the FT/GFA(r) model are rather accurate, at least, for the engineering practice. For the above range any signs of the singularity with the exponent $(1-\alpha)$ are not observable in the described approach.

Douslin and Harrison [10] reported the empirical (with the nonuniversal exponent β) CXC fit in terms of two asymmetric i variants of Eq. (12):

$$\bar{\rho}_i = \pm B_0 \bar{T}^\beta + D_i \bar{T}. \tag{32}$$

The results of such treatment [similar to that used in the GFA(s) model] are represented in Table III and shown in Fig. 6. In spite of the consistent approach to the CXC fit based in [10], simultaneously, on the careful analysis of $\rho_d^*(T)$ and $A_\sigma(T)$ behavior, one may note the same evident shortcoming existing in the CXC fit for CO_2 (see Table IV) proposed by Michels *et al.* [31]. This is an unsatisfactory description of the

TABLE III. Critical parameters, exponents and CXC amplitudes used by Michels *et al.* for CO_2 [31] and by Douslin and Harrison for C_2H_6 [10] in comparison with the reanalyzed description based on the GFA(r) model (see Figs. 6 and 7).

CO_2 [31]	$T_c = 304.19$ K; $P_c = 7.381$ MPa; $\rho_c = 10.6136\ \mathrm{g/cm^3}$; $Z_c = 0.275$
CXC fit [31]	$B_o = 2.0754$; $D_1 = 0.9618$; $\beta = 0.357$; $A_c = 6.625$
GFA(r)	$B_o = 1.9169$; $D_1 = 0.9169$; $\varepsilon = 0.01$; $k = 4$; $A_c = 7.044$ [32]
FT (T_C) [6]	$a_c{}^o = 196.58\ \mathrm{J\ dm^3/mol^2}$; $b_c{}^o = 0.03141\ \mathrm{dm^3/mol}$; $1 - c_c{}^o = 0.7333$
C_2H_6 [10]	$T_c = 305.33$ K; $P_c = 4.8717$ MPa; $\rho_c = 6.87\ \mathrm{mol/dm^3}$; $Z_c = 0.2793$
CXC fit [10]	$B_o = 1.7224$; $D_1 = 0.7889$; $D_l = 0.7566$; $D_g = 0.8222$; $\beta = 0.35$
GFA(r)	$B_o = 1.8566$; $D_1 = 0.8933$; $\varepsilon = 0.015$; $k = 2$; $A_c = 6.4$ [10]
FT (T_C) [8]	$a_c{}^o = 309.66\ \mathrm{J\ dm^3/mol^2}$; $b_c{}^o = 0.048\ 52\ \mathrm{dm^3/mol}$; $1 - c_c{}^o = 0.7449$

TABLE IV. Comparison of CXC fit for CO_2 [31] with the experimental orthobaric data and the prediction obtained by the FT/GFA(r) model (see text).

T, K	$\delta\rho_l$ (%) [31]	$\delta\rho_l{}^F T$ (%)	$\delta\rho_g$ (%) [31]	$\delta\rho_g{}^F T$ (%)	δP_σ (%) Eq. (29)	$\delta P_\sigma{}^F T$ (%) [31]	$\delta P_\sigma{}^F T$ (%)
276.003	1.33	− 0.92	− 11.8	− 0.75	− 0.01	− 1.04	− 1.63
283.972	1.12	− 0.69	− 7.13	− 0.11	0.33	− 1.20	− 1.28
293.024	0.77	− 0.37	− 3.63	0.17	0.48	− 0.98	− 0.88
298.220	0.59	− 0.01	− 1.83	0.68	0.44	− 0.71	− 0.40
298.448	0.66	0.09	− 2.04	0.41	0.43	− 0.56	− 0.37
301.202	0.46	0.29	− 1.25	0.75	0.19	− 0.37	− 0.12
303.079	0.92	1.10	− 0.54	1.34	0.04	− 0.13	0.14
303.559	0.34	0.62	0.45	− 1.61	0.01	− 0.18	− 0.45
304.163	− 1.82	1.05	1.27	0.04	− 0.09	− 0.02	− 0.02
304.190	0	0	0	0	0	0	0

vapor density at the lower temperatures (Fig. 6). The relative deviations $\delta\rho_g$ for C_2H_6 have the same sign as those for CO_2 and become here systematic.

Since the g branch provides the main information at the calculation of both (nonclassical $P_\sigma[\rho_g(T)]$ and classical $P_\sigma^0[\rho_g(T)/\rho_l(T)]$) FT functionals, we have used for C_2H_6 the same universal GFA(r) methodology developed above for CO_2. The crucial step is the choice of $A_c = 6.4$ (the asymptotic value predicted by the analytic Cox's equation for $P_\sigma(T)$ [10]) verified before [8] by the FT model. The amplitudes B_0, D_1 and the GFA(r) parameters (ε, k) given in Table III provide the reliable description of g branch as shown in Fig. 6.

The most intriguing result of the FT model is, of course, a prediction of two close but separate branches, $P_\sigma(T) \leqslant P_\sigma^0(T)$ (Fig. 7), which are represented, respectively, by the dew point's $P_\sigma[\rho_g(T)]$ functional [Eq. (29)] and by the bubble point's $P_\sigma^0[\rho_g(T)/\rho_l(T)]$ functional. This distinction for a pure substance bears the strong resemblance with the well-known shape of the (P,T) projection for a mixture of constant composition. The nonanalytic asymptotic crossing of the above branches exists at the critical point itself. It corresponds to the *critical crossover from the classical l branch* with its larger bubble point's pressure $P_\sigma^0(T)$ *to the nonclassical g branch* with its dew-point's pressure $P_\sigma(T)$. Only the latter is experimentally detectable while the former is the internal pressure of l phase at which the first stable bubbles can be formed. The latent (classical) heat $r_0(T)$ of such onset of the vaporization is the slightly less than the nonclassical heat $r(T)$ of condensation following from the differential Clapeyron's Eq. (9).

The GFA phenomenology rejects the classical concept of unified EOS. Such an approach may be important to develop the nonclassical nucleation theory [30] in which the dynamics of vaporization and condensation is essentially different. It should be noted that the scaling analysis of an asymptotic supercritical behavior of mixtures at the infinite dilution

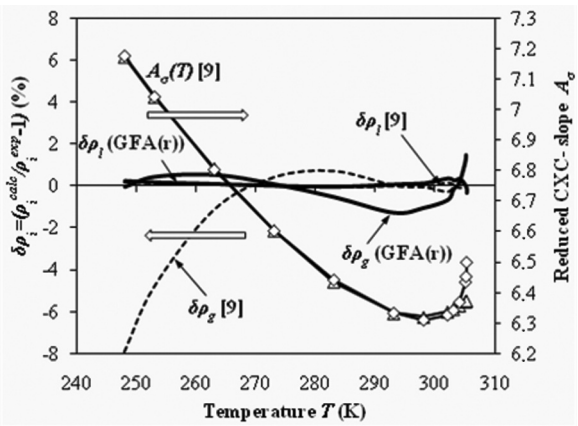

FIG. 6. Trends of the percentage differences (left scale for $\delta\rho_i$) between the experimental CXC densities ρ_i ($i = l$ or g) obtained by Douslin and Harrison [10] (zero axis) for ethane and the values of CXC fit [10] (dotted lines) in comparison with those calculated by the GFA(r) model (solid lines). Two variants of $A_\sigma(T)$ approximation (right scale for A_σ) by the analytic Cox's equation (triangles) [10] and nonanalytic Goodwin's equation (diamonds) [10] are shown too (thin lines). *Both demonstrate the* A_σ *minimum at* $T_m \approx 298$ K *observable also in many other substances* [6–8] *near the critical points.*

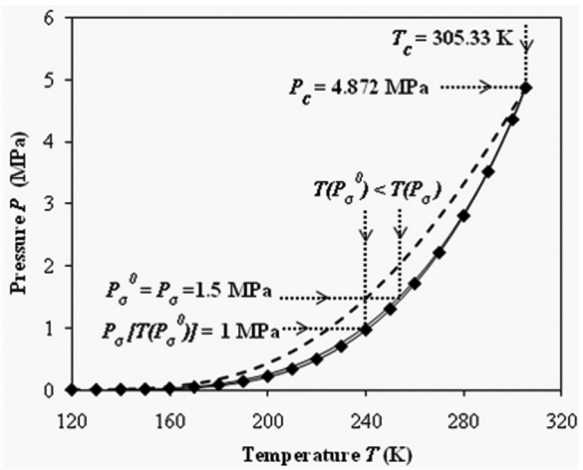

FIG. 7. The quantitative prediction by the FT model of the (v,l)-*interphase* region located between the measurable dew point's (solid line) $P_\sigma[\rho_g(T)]$ *curve and the supposed bubble point's (dashed line)* $P_\sigma{}^o[\rho_g(T)/\rho_l(T)]$ curve (see text) and comparison with the experimental vapor-pressure data (diamonds) for ethane [10]. The arbitrary chosen subcritical isotherm and isobar (thin dotted lines with arrows) demonstrate (presumably) vaporization of classical liquid and condensation of nonclassical (essentially inhomogeneous) vapor, respectively (see, for comparison, Fig. 3 in [2]).

reported by Levelt Sengers [35] confirms just the described beaked shape (Fig. 7) of (*P*,*T*) projection in the very vicinity of a solvent's critical point. The reliable predictive ability (see Table III for CO_2) of FT functional $P_\sigma[\rho_g(T)]$ follows also from Fig. 7. The GFA(r) model provided the input $\rho_g(T)$ data for C_2H_6 and the deviations between the predicted and experimental [10] P_σ values were less than 0.5 bar at the lowest temperature $T = 248.15$ K. One may note that the distinction in the critical slope A_c of nonanalytic (6.5) and analytic (6.4) variants of $P_\sigma(T)$ description discussed in [10] is negligible.

V. THERMODYNAMIC NATURE OF DISTINCTIONS BETWEEN VDW-LIKE AND ISING-LIKE CLASSES OF CRITICAL UNIVERSALITY

The origin of nonanalyticity in real fluids is especially obvious from Figs. 1 and 7. The split of single measurable vapor-pressure curve $P_\sigma(T)$ onto two branches [$P_\sigma(T)$ itself and $P^0_\sigma(T)$] gives rise to the existence of a third *interphase* located at any subcritical temperature between the stable *g*- and *l*-bulk phases. This term is not equivalent of the standard one (*interface*) in which the equality of bulk pressures, $P_g = P_l = P_\sigma$, is supposed while the imbalance with the model tangential pressure $P_{xy}(z)$ exists. It determines the surface tension $\gamma_\sigma(T)$ by the integrable functional [36]:

$$\gamma_\sigma = \int_{-\infty}^{+\infty} [P_\sigma - P_{xy}(z)]dz. \tag{33}$$

By contrast, the concept of *interphase* well defined here is completely consistent with the measurable CXC properties [$P_\sigma(T)$, $\rho_g(T)$, $\rho_l(T)$] but implies the certain shifts of fields, $\Delta P_\sigma = P^0_\sigma - P_\sigma$ and $\Delta\mu_\sigma = \mu^0_\sigma - \mu_\sigma$, at each subcritical temperature excepting the critical one. One may suppose the existence of small "field glides" between two stable phases. Hence, *there is nothing thermodynamically unusual about the existence of two trend's singularity in a critical point itself.*

The relevant questions were discussed recently by Wang and Anisimov [13] to map the asymmetric criticality of real fluids into the symmetric Ising-like criticality. The promoted methodology was a search for an appropriate mixing of the reduced thermodynamic fields,

$$\hat{T} = T/T_c,\ \hat{\mu} = \mu/k_BT_c,\ \hat{P} = P/\rho_c k_B T_c = Z_c P/P_c, \tag{34}$$

into the complete scaling's fields [14]. The chosen scales of μ and P either imply critical values,

$$\mu_c = k_BT_c; \quad P_c = \rho_c k_B T_c\ (Z_c = 1), \tag{35}$$

in the lattice-gas model where a linear approximation for the dependent field $\hat{P}(\hat{\mu},\hat{T})$ is used,

$$\frac{P - P_\sigma}{\rho_c k_B T_c} = \Delta\hat{P} = \left(\frac{\partial\hat{P}}{\partial\hat{T}}\right)_{\Delta\hat{\mu}=0}\Delta\hat{T}, \tag{36}$$

or suppose the asymptotic proportionality expressed here in terms of the difference variables,

$$\bar{P}_\sigma = 1 - P_\sigma/P_c = (s_c/k_BZ_c)\,\bar{T}. \tag{37}$$

One obtains by its differentiation asymptotically:

$$s_c/k_B = A_cZ_c. \tag{38}$$

Substitution into Eq. (10) confirms just the one trend's nature of the asymptotic scaling criticality:

$$\Delta\bar{\rho} = \frac{\rho_l - \rho_g}{2\rho_c} = \frac{s_g - s_l}{2s_c} = \Delta\bar{s}k_B/s_c. \tag{39}$$

The thermodynamically arbitrary value of specific critical entropy [13] is now exactly determined by Eq. (38). Let us remember, however, that the more general two-trend's approach realizable in the FT model requires also the alternative determination,

$$s^0_c/k_B = A^0_cZ_c = 4Z_c, \tag{40}$$

at the same critical point of the classical *l* branch in real fluids (Fig. 7). This uncertainty in the determination of critical entropy exists at any analytic or nonanalytic fit of the actual slope A_c. It cannot be eliminated in the framework of two trend's approach.

Understandably, in the FT model two system-dependent amplitudes (B_0, D_1) or, equivalently, (A_c, D_1) play the same role as those (A^-_0, B_0) used to describe the local singularity of the CXC diameter (see Table I). Unfortunately, it is hard to compare experimentally such results since none of the three standard heat capacities C_v, C_P, C_σ can conveniently be measured directly for a liquid on its saturation curve [36]. The similar situation is observable in the two-phase region where the scarce available heat-capacity data are seldom accurate enough to estimate reliably the amplitudes and the analytical "critical-background" term $\hat{B}_c$ [13]:

$$\hat{C}_v = A^-_0|\Delta\hat{T}|^{-\alpha}(1 + A^-_1|\Delta\hat{T}|^{\Delta}) - \hat{B}_c. \tag{41}$$

This (modified by the mean-field-contribution) Wegner's-type form corresponds to the similar mod-ification (13) adopted for the CXC diameter [13]. As a result, the amplitude,A^-_0, is proportional to the amplitude D_0, the amplitude B^2_0 is proportional to the amplitude D_2, and the critical-background term $\hat{B}_c$ is proportional to the amplitude D_1.Wang and Anisimov [13] have supposed the poss-ible compensation of both singular contributions in Eq. (13) for a set of normal substances:

$$D_0\bar{T}^{1-\alpha} = D_2\bar{T}^{2\beta}. \tag{42}$$

To illustrate the predictive ability of the FT model in the near-critical region of liquidus states at $\rho > \rho_c$ the evaluated values of amplitudes are represented in Table V.

Some comments about Tables I and V are necessary. The *two-scale-factor universality principle* discussed by many authors [2,13,17,37] adopts the existence of *two independent* amplitudes just as there are *two independent* exponents. The classical *corresponding states principle* admits [29] the existence of linear interrelation between the main criteria (Z_c, A_c) of thermodynamic similarity. The simplified FT estimates of amplitudes (A^+_0, A^-_0) in Tables I and V are based on this admission but its approximate value follows from the column $\pm(A_cZ_c)^{-1}$ representing asymptotic slopes in Fig. 1. Nevertheless, their agreement with the (scarce and scattered) experimental data collected, for example, in [17] (for Ar, $A^+_0 = 1.88$ or 2.0, $A^-_0 = 4.52$ or 4.03; for C_2H_6, $A^+_0 = 2.22$, $A^-_0 = 4.09$: for CO_2, $A^+_0 = 2.43 - 3.06$, $A^-_0 = 5.32 - 5.56$) looks to be reasonable. The predicted FT amplitude B_0 is larger than that for C_2H_4 ($B_0 = 1.642$) and C_2H_6 ($B_0 = 1.649$) but

TABLE V. Criteria of similarity and amplitudes predicted by the FT model at sub- and supercritical temperatures of liquidlike densities $\rho > \rho_c$ (for FT exponents, see Table I).

Fluid	Z_c	A_c	$\pm(A_cZ_c)^{-1}$	$B_0 = A_c{}^{1/3}$	$\approx A_0{}^+$	$\approx A_0{}^- = B_0A_0{}^+$
vdW	3/8	4	2/3	1.5873	1.41	2.24
Ar [6]	0.2919	5.943	0.5764	1.8113	2.07	3.75
C_2H_4 [6]	0.2812	6.354	0.5597	1.8522	2.20	4.07
C_2H_6	0.2793	6.400	0.5594	1.8566	2.22	4.11
CO_2	0.2745	7.044	0.5172	1.9169	2.33	4.46
H_2O [6]	0.2292	7.860	0.5551	1.9883	2.89	5.75
Rb	0.2173	11.27	0.4083	2.242	3.44	7.71
Cs	0.2028	11.39	0.4329	2.250	3.70	8.32

smaller for H_2O ($B_0 = 2.035$) from [13]. The predicted FT amplitudes A_0^- are systematically less than that from [13] [fitted to Eq. (41)]. However, the difference between the amplitude A_0^- for C_2H_6 and H_2O (2,16) is similar to that (1,64) following from Table V.

One may note that the ratio of amplitudes in the FT model is substance dependent, $A_0^+/A_0^- = 1/B_0$, as the result of GFA while it is universal [2,13,38], $A_0^+/A_0^- = 0.523$, in the Ising-like systems. It is worthwhile also to note that the universal FT combination of amplitudes and exponents $(\alpha', A_0^-, C_0, B_0)$ is fulfilled as the equality (Table I) $\alpha'\beta = 1/18$ only along the orthobaric l branch while in the supercritical region of densities $\rho > \rho_c$ it becomes for amplitudes and exponents $(\alpha', A_0^+, C_0, B_0)$ substance dependent with the same B_0^{-1} factor: $\alpha'\beta/B_0$.

Another interesting feature is the *exact* coincidence of three FT exponents from Table I (α, β, γ) with those following [39] from the Ising type of EOS *in the one-loop approximation*. However, the fourth experimentally most problematic exponent $\delta = 4$ [39] as well as the hyperscaling one $\eta = 0$ are significantly different from the respective FT estimates ($\delta = 9/2, \eta = 1/11$). One may notice that the 3/2 law expressed by Eq. (1e) is approximately fulfilled ($\beta\delta = 1.565$) for the best Ising-like exponents (Table I) but it fails for the above quantity $\delta = 4$. The possible interpretation of such a discrepancy can be obtained phenomenologically in the framework of the well-known Fisher's droplet model [18,40], for example, combined with the FT model's results. Indeed, there is a sort of complementarity between both approaches. The former provides the adequate description of g branch in terms of two normalization exponents (σ, τ) but predicts a variety of "pathological" shape for l branch [40]. The latter, on the contrary, guarantees the reliable representation of l branch but demonstrates the existence of some narrow one-phase strip of anomalous behavior in the vicinity of g branch discussed below. In both approaches the adopted existence of heterophase fluctuations just in the near-critical gaseous ($\rho < \rho_c$) states is the determinative physical concept.

The split of the phase boundary in the field (P, μ, T) space (Fig. 7) predicted by the FT model and the argued existence of a third *interphase* in addition to the stable bulk phases of liquid and gas make the vdW-like problem of metastability completely nontrivial. While its classical variant [38] is based on the concept of a unified (cubic) EOS with the well-defined locations of *binodal* (Fig. 1) and *spinodal*, we have demonstrated the failure of this methodology *along the entire CXC range for real fluids*. The same format of cubic FT-EOS but with the different sets of T-dependent coefficients was used to reconstruct reliably the one-phase behavior of both stable regions on the thermodynamic surface of equilibrium states. Such an approach provides the accurate location of phase boundary (the input CXC data) and simultaneously it predicts the shape of nonclassical and classical spinodals which determine the metastable regions of both phases (Figs. 8 and 9).

The accurate shapes of predicted loci are shown for CO_2 in the (T,ρ) plane (Fig. 8) and in the (P,T) plane (Fig. 9). The unique envelope of all classical subcritical isotherms determines in the (P,ρ) plane the boundary of interphase expressed by Eq. (29) written for the critical isotherm T_c, which coincides with the dew point's branch of CXC. The ordinary nonclassical isotherm $T < T_m$ located outside the CXC must have a finite jump (discontinuity) in the isothermal compressibility when it attains the $P_\sigma(\rho_g)$ parameters of a respective dew point. This situation resembles the main feature of *second-order phase transition.* It is different from the

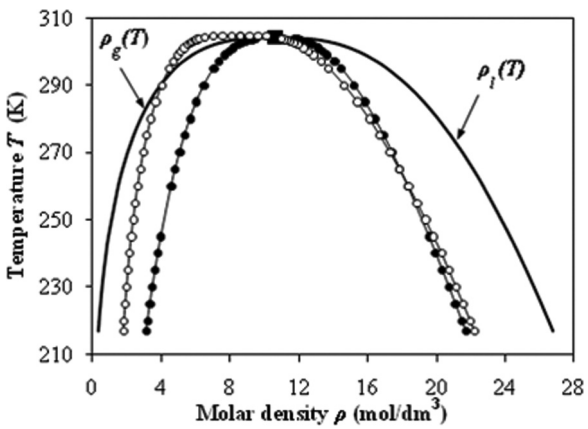

FIG. 8. Comparison of the nonclassical (open circles) and classical (solid circles) branches of FT spinodal for CO_2; the input orthobaric densities [32] are shown by solid lines. The anomalous strip of heterophase fluctuations located between the nonclassical spinodal and the input orthobaric vapor density $\rho_g(T)$ at the upper temperatures ($T \geqslant T_m \approx 292$ K) contains the family of near-critical isobars with the slight positive slope $(\partial T/\partial\rho)_p(\alpha_p < 0)$. The spectacular fluctuational flattening of nonclassical spinodal in comparison with its classical counterpart (shown by thin line with black symbols) is evident.

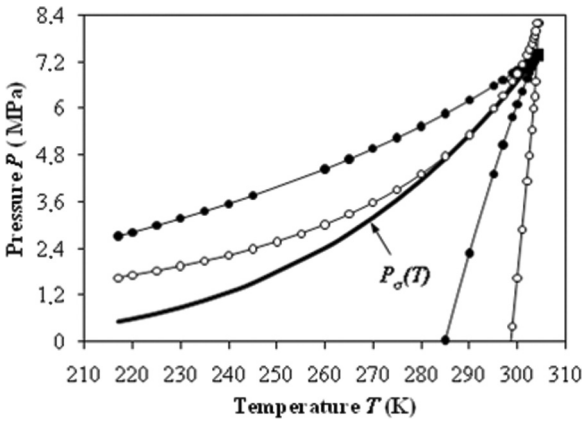

FIG. 9. Comparison of the nonclassical (open circles) and classical (solid circles) spinodals with the input [32] vapor-pressure curve $P_\sigma(T)$ (solid line) for CO_2 demonstrates the anomalous near-critical behavior of the nonclassical spinodal's branch. It is tangential to the vapor-pressure curve just at temperature $T_m \approx 292$ K and, then, predicts the unwanted large supersaturation of nonclassical vapor at the near-critical temperatures.

both classical concepts of *metastability* and the *first-order phase transition*. One usually adopts that the isothermal compressibility (and the Gaussian fluctuations of overall average density) remains the continuous function of density along the metastable extension of subcritical isotherm into the two-phase region. On the other hand, this response function must be formally divergent if the concept of first-order transition in the infinite-volume system is realized in terms of an isotherm-isobar coincidence. Such coincidence is absent in the *interphase* predicted by the FT model. The certain decrease of compressibility at the ordinary transition $T < T_m$ into the two-phase region from the side of nonclassical gas designates [30] the onset of heterophase *equilibrium* nucleation (condensation). The isothermal slope $(\partial P/\partial\rho)_T$ becomes also (see Fig. 8) the negative in the anomalous strip of near-critical states ($T \geqslant T_m$). The respective g states located outside but close to the dew point's branch $P_\sigma(\rho_g)$ cannot be stable and the probability of dropletlike heterogeneous structure becomes here obvious. Just such peculiarity of near-critical vapor states has been admitted by the known Fisher's droplet model [40].

The behavior of nonclassical isobars within the near-critical range $[T_m, T_c]$ is especially interesting. While the classical critical isotherm demonstrates the inflection at the *actual* critical point in the (P,ρ) plane, the nonclassical critical FT isobar attains only the maximum at the *actual* critical point in the (T,ρ) plane. Its other spinodal point (the minimum) is located in the anomalous near-critical gas. The very small negative slope of anomalous nonclassical isobars exists outside the dew-point's branch and disappears only at the T_m point, where the nonclassical spinodal coincides with the CXC (Fig. 8). It *touches* the vapor-pressure curve $P_\sigma(T)$ just at the T_m point in the P,T plane (Fig. 9). Such unusual shape of nonclassical FT spinodal predicts the possibility to reach the very high degree of supersaturation for the nonclassical metastable g phase just in the anomalous near-critical range $[T_m, T_c]$. Obviously, that the presence of metastable gaslike states may be the misrepresenting factor at the experimental estimate of exponent δ. As a result, the classical liquid can demonstrate the scaling Ising-like properties only within the very narrow asymptotic range.

VI. CONCLUSIONS

The GFA methodology promotes in the framework of the FT model the rather radical hypothesis of vdW-like universality which does not need the subdivision of local thermodynamic potentials into the Ising-like critical term and the analytical background contribution. Such separation cannot be reasonably unambiguous, at least, along the CXC for the whole range of subcritical temperatures where the both (singular and linear) terms in Eq. (12) are essential. The GFA methodology developed here is in agreement with the suggestion formulated by Moldover and Gammon [37] that the measured near-critical density of the vapor $\rho_g(T)$ might be too high (Sec. II) (because of a wetting layer on the inside of the cell) to cause the $(1-\alpha)$ singularity found in such substances as SF_6 [20,22]. Presumably, this Ising-like singularity is not the inherent property implied by the structure of real fluids. Such a conclusion can be extended to the CXC description of liquid metals too. The conventional amplitudes A_0^-, D_0, D_2 have not been used in the formulation of GFA models which are based on the hypothesis of vdW-like universality with the well-determined and measurable amplitudes: B_0, A_c, D_1.

The well-known (with the δ exponent supposed by scaling) monotonous behavior of nonclassical critical isotherm in the (P,ρ) plane (non-negative slope) is difficult to achieve from the *equilibrium* experiments. If the scaling results of Ising-like universality are well-determined *above* T_c, the postulated "longitudinal" symmetry of $C_v(\rho_c, T)$ *below* T_c as well as the "transversal" symmetry of $\beta_T[\rho_i(T)]$ along the both orthobaric branches need the further investigation.

It is worthwhile to remember that the asymmetric (with the odd degrees of local density) variant of the Landau-Ginzburg-Wilson Hamiltonian introduced by Nicoll [41] leads to the $(1-\alpha)$ singularity of CXC diameter as well as to the non-mean-field type of EOS which is close inherently to that obtained in the framework of complete scaling [42]. The former approach develops, in fact, the well-known concept of the continuous interface profile formulated by vdW himself in terms of the Helmholtz-energy-density functional and the respective gradient of density. The underlying feature usable in Eq. (33) is the supposed possibility to describe the both coexisting phases by the *unified* EOS (mean-field [36] or non-mean-field [38,41,42]).

The FT model leading to the concept of GFA is an attempt to go beyond the constraint of unified EOS and to obviate its consequences. In particular, it proves that the *vdW-classical reduced slope* $A_c^0 = 4$ *is essential together with the real slope* A_c in the vicinity of the *actual* critical point $(T_c, \rho_c, P_c; Z_c)$. On the other hand, it is straightforward to demonstrate that the *local* interpretation of FT-EOS [7] as a unified EOS with the constant *actual* critical slope A_c leads, at once, to the odd cubic contribution ($\sim \bar{T}\bar{\rho}^3$), which is absent in the original vdW-EOS [2]. This assumption is similar to that expressed by Eq. (37) in

the one-trend consideration of criticality [13]. Such interrelation between the theoretically based and phenomenological approaches is very interesting and needs, to our mind, further investigation.

[1] L. Cailletet and E. Matthias, C. R. Acad. Sci. **112**, 1170 (1891).
[2] A. K. Wyczalkowska, J. V. Sengers, and M. A. Anisimov, Physica A **334**, 482 (2004).
[3] K. G. Wilson, Phys. Rev. B **4**, 3174 (1971).
[4] M. E. Fisher, Rev. Mod. Phys. **46**, 597 (1974).
[5] F. J. Wegner, Phys. Rev. B **5**, 4529 (1972).
[6] V. B. Rogankov and L. Z. Boshkov, Phys. Chem. Chem. Phys. **4**, 873 (2002).
[7] V. A. Mazur and V. B. Rogankov, J. Mol. Liq. **105**, 165 (2003).
[8] V. B. Rogankov, O. G. Byutner, T. A. Bedrova, and T. V. Vasiltsova, J. Mol. Liq. **127**, 53 (2006).
[9] S. Jüngst, B. Knuth, and F. Hensel, Phys. Rev. Lett. **55**, 2160 (1985).
[10] D. R. Douslin and R. H. Harrison, J. Chem. Thermodyn. **5**, 491 (1973).
[11] N. D. Mermin, Phys. Rev. Lett. **26**, 957 (1971).
[12] N. D. Mermin and J. J. Rehr, Phys. Rev. Lett. **26**, 1155 (1971).
[13] J. Wang and M. A. Anisimov, Phys. Rev. E **75**, 051107 (2007).
[14] Y. C. Kim, M. E. Fisher, and G. Orkoulas, Phys. Rev. E **67**, 061506 (2003).
[15] V. B. Rogankov, High Temp. **47**, 656 (2009).
[16] V. B. Rogankov, V. I. Levchenko, and Y. K. Kornienko, J. Mol. Liq. **148**, 18 (2009).
[17] D. Broseta, Y. Melean, and C. Miqueu, Fluid Phase Equilib. **233**, 86 (2005).
[18] M. E. Fisher, J. Stat. Phys. **75**, 1 (1994).
[19] K. S. Pitzer, J. Phys. Chem. **99**, 13070 (1995).
[20] J. Weiner, K. H. Langley, and N. C. Ford, Jr., Phys. Rev. Lett. **32**, 879 (1974).
[21] E. T. Shimanskaya, I. V. Bezruchko, V. I. Basok, and Y. I. Shimanskii, Sov. JETP **53**, 139 (1981).
[22] B. J. Thijsse, J. Chem. Phys. **74**, 4678 (1981).
[23] L. Luettmer-Strathmann, S. Tang, and J. V. Sengers, J. Chem. Phys. **97**, 2705 (1992).
[24] V. B. Rogankov and T. A. Bedrova, in *Vestnik Lvivskogo Universiteta*, Vol. 38 (Lviv University Publications, Ukraine, 2005), p. 197.
[25] M. W. Pestak, R. E. Goldstein, M. H. W. Chan, J. R. de Bruyn, D. A. Balzarini, and N. W. Ashcroft, Phys. Rev. B **36**, 599 (1987).
[26] J. S. Rowlinson, Nature (London) **319**, 362 (1986).
[27] R. E. Goldstein and N. W. Ashcroft, Phys. Rev. Lett. **55**, 2164 (1985).
[28] R. R. Singh and K. E. Pitzer, J. Chem. Phys. **92**, 3096 (1990).
[29] L. P. Filippov, *Methods of Calculation and Prognosis for Properties of Substances* (Moscow University Publications, Moskow, 1988).
[30] V. B. Rogankov, in *Nucleation Theory and Applications,* edited by J. W. P. Schmelzer, G. Röpke, and V. B. Priezzhev, Vol. XIII (Joint Institute of Nuclear Researches Publ., Dubna, 2011), p. 225.
[31] A. Michels, B. Blaisse, and C. Michels, Proc. R. Soc. London A **160**, 358 (1937).
[32] W. Duschek, R. Kleinrahm, and W. Wagner, J. Chem. Thermodyn. **22**, 841 (1990).
[33] Z. Y. Chen, P. C. Albright, and J. V. Sengers, Phys. Rev. A **41**, 3161 (1990).
[34] D. G. Friend, H. Ingham, and J. F. Ely, J. Phys. Chem. Ref. Data **20**, 275 (1991).
[35] J. M. H. Levelt Sengers in *Supercritical Fluids,* edited by E. Kiran and J. M. H. Levelt Sengers (US Government, Netherlands, 1994).
[36] J. S. Rowlinson, *Liquids and Liquid Mixtures* (Batherworth Science, London, 1969).
[37] M. R. Moldover and R. W. Gammon, J. Chem. Phys. **80**, 528 (1984).
[38] M. E. Fisher and S.-Y. Zinn, J. Phys. A: Math. Gen. **31**, L629 (1998).
[39] S. K. Ma, *Modern Theory of Critical Phenomena* (Westview Press, Boulder, CO, 1976).
[40] M. E. Fisher, Physics (N.Y.) **3**, 255 (1967).
[41] J. F. Nicoll, Phys. Rev. A **24**, 2203 (1981).
[42] C. E. Bertrand, J. F. Nicoll, and M. A. Anisimov, Phys. Rev. E **85**, 031131 (2012).